PHYSICAL REVIEW B **85**, 060506(R) (2012)

Absolute value and temperature dependence of the magnetic penetration depth in $Ba(Co_{0.074}Fe_{0.926})_2As_2$

Oren Ofer,[1,*] J. C. Baglo,[2] M. D. Hossain,[2] R. F. Kiefl,[2,3] W. N. Hardy,[2] A. Thaler,[4] H. Kim,[4] M. A. Tanatar,[4] P. C. Canfield,[4] R. Prozorov,[4] G. M. Luke,[5] E. Morenzoni,[6] H. Saadaoui,[6] A. Suter,[6] T. Prokscha,[6] B. M. Wojek,[6,7,†] and Z. Salman[6]

[1]*TRIUMF, 4004 Wesbrook Mall, Vancouver, British Columbia, Canada V6T 2A3*

[2]*Department of Physics and Astronomy, University of British Columbia, Vancouver, British Columbia, Canada V6T 1Z1*

[3]*Canadian Institute for Advanced Research, Toronto, Ontario, Canada M5G 1Z8*

[4]*Ames Lab and Department of Physics and Astronomy, Iowa State University, Ames, Iowa 50011, USA*

[5]*Department of Physics and Astronomy, McMaster University, Hamilton, Ontario, Canada L8S 4M1*

[6]*Laboratory for Muon-Spin Spectroscopy, Paul Scherrer Institute, CH-5232 Villigen PSI, Switzerland*

[7]*Physik-Institut der Universität Zürich, Winterthurerstrasse 190, CH-8057 Zürich, Switzerland*

(Received 6 February 2012; published 28 February 2012)

The absolute value and temperature dependence of the in-plane magnetic penetration depth λ have been measured on a single crystal of $Ba(Co_{0.074}Fe_{0.926})_2As_2$ using low-energy muon-spin rotation and microwave cavity perturbation. The magnetic field profiles in the Meissner state are consistent with a local London model beyond a depth of 15 nm. We determine the gap symmetry through measurements of the temperature dependence of the superfluid density which follows a two-gap s-wave model over the entire temperature range below T_c. While the intermediate to high temperature data is well fit by an energy gap model in the BCS-like (weak-coupling) limit, a second smaller gap becomes apparent at low temperatures.

DOI: 10.1103/PhysRevB.85.060506 PACS number(s): 74.70.Xa, 74.25.Ha, 76.75.+i

The discovery of high-T_c superconductivity in iron-based materials[1,2] has motivated a large number of scientific studies. The most striking similarity with the cuprates is the close proximity between superconductivity and magnetism as a function of chemical composition. However, there are also considerable differences, particularly with regard to how changes in the composition lead to superconductivity. In the cuprate superconductor $YBa_2Cu_3O_{7-\delta}$ (YBCO), doping originates in the CuO chains which are adjacent to the active CuO_2 layers. To a first approximation the chains control the hole doping of the CuO_2 planes without altering the structure of the planes. On the other hand, in $Ba(Co_xFe_{1-x})_2As_2$ the Co replaces Fe in the active Fe_2As_2 layers. Thus, in addition to changing the carrier concentration, the Co must have a direct effect on the band structure[3] and is an intrinsic source of scattering. Furthermore, in the pnictides there seem to be considerable differences in the phase diagrams depending on the system. For instance, in $LaO_{1-x}F_xFeAs$,[4] the doping-induced transition between antiferromagnetism and superconductivity appears discontinuous as in a first-order transition. In contrast, $Ba(Co_xFe_{1-x})_2As_2$ is more similar to the cuprates, where the antiferromagnetic phase is suppressed gradually as a function of doping.[5] Careful comparisons of the two families and compounds within each family may help identify essential factors that give rise to high-T_c superconductivity (for a review, see Refs. 6 and 7).

One of the most important experimental observables in any superconductor is the magnetic penetration depth λ since it is directly related to the superfluid density $\rho \propto 1/\lambda^2$ and hence to the magnitude of the superconducting order parameter. Its variation as a function of temperature, composition, and magnetic field provides important tests for any model of superconductivity. For example, the temperature dependence $\lambda(T) = \lambda(0) + \Delta\lambda(T)$ can distinguish between some pairing symmetries, e.g., d and s wave. In a clean d-wave superconductor, $\rho(T)$ is linear at low temperatures, as found in YBCO.[8,9] On the other hand, in an s-wave superconductor one expects an isotropic energy gap and a resulting exponential suppression of $\Delta\lambda(T)$ at sufficiently low T. Such studies require accurate measurements of the absolute value of λ, which are difficult. One source of systematic error is the uncertainty regarding the form of the magnetic field profile in either the Meissner state or the vortex state.[10] For example, it is often assumed that the field profile near the surface in the Meissner state is simply exponential, whereas this is only strictly valid in the case of a perfectly flat surface of a nonmagnetic sample with an order parameter that is depth invariant. Any deviations from this ideal situation add uncertainty to measurements of λ and $\Delta\lambda(T)$. Measurements in the vortex state are free of any surface problems but depend on the vortex lattice geometry, the vortex structure, and the vortex interactions. Vortex lattice disorder, if it is large, is particularly problematic.[11,12]

In this Rapid Communication we report precise measurements of the in-plane penetration depth in the Meissner state on a single crystal of $Ba(Co_{0.074}Fe_{0.926})_2As_2$. The results strongly support a two energy-gap model. The measurements were performed using a combination of low-energy muon-spin rotation (LE-μSR) and microwave cavity perturbation. LE-μSR provides a precise determination of the absolute value of λ, whereas microwave measurements are very sensitive to relative variations of this quantity with temperature. The combination of the two techniques allows a precise determination of the T dependence of the magnetic penetration depth and superfluid density, which depend on the symmetry of the superconducting gap. The Meissner state measurements presented here avoid many of the potential uncertainties described above.

There have been numerous studies on this system[13–20] using other methods but there is no consensus on the pairing symmetry. Heat transport studies have not reached a consensus on the superconducting gap structure, with some studies

suggesting a nodeless gap in the *ab* plane[14] pointing to a two-gap *s*-wave model, while others suggest a nodeless gap only at optimal doping but gap nodes elsewhere.[15] Magnetic force microscopy (MFM),[16,17] microwave,[18] and tunnel diode resonator (TDR) measurements[5,19,20] show that the magnetic penetration depth $\lambda(T)$ follows a weak power-law behavior, with $\Delta\lambda(T) \propto T^m$, with $2 \leqslant m \leqslant 2.5$, depending on the doping. In the current study we measure the field profile directly on a freshly cleaved surface of $Ba(Co_{0.074}Fe_{0.926})_2As_2$. We find that beyond 15 nm the magnetic field falls exponentially as a function of depth with an extrapolated $\lambda(0) = 250(8)$ nm. The temperature dependence of the superfluid density is obtained by combining LE-μSR and microwave resonance data on the same crystal. Significant differences are observed in the low-temperature behavior of λ compared with other techniques on different crystals, suggesting that the spectrum of low-energy excitations depends sensitively on the surface characteristics.

The single crystal of optimally doped $Ba(Co_{0.074}Fe_{0.926})_2As_2$ was grown using a self-flux method.[21] The crystal was approximately square shaped with dimensions 9 mm × 9 mm × 0.5 mm and exhibited a sharp transition at $T_c = 21.7$ K [with 0.8(2) K width] as measured by superconducting quantum interference device (SQUID) magnetometry. The crystal was attached to a high-purity Al sample holder coated with 1 μm of Ni, which suppresses any background precession signal from muons missing the sample.[22] The crystal was cleaved to a thickness of about 0.3 mm under flowing N_2 gas just prior to loading it into the ultrahigh-vacuum sample chamber. The high-intensity μE4 muon beam line at the Paul Scherrer Institute in Switzerland[23] provides a beam of low-energy muons at a rate of about 10^4 s^{-1}, which uses a solid Ar moderator capped with a layer of N_2. Low-energy muons are emitted from the moderator and accelerated to 15 keV before being transported electrostatically to the μSR spectrometer. Muons are implanted in the sample with an energy which can be controlled by a voltage applied to the sample holder. Further details on the spectrometer and technique are given elsewhere.[24] Implantation profiles for each energy are calculated using the Monte Carlo code TRIM.SP (Ref. 25) taking into account the spread in energy and incident angle of the muon beam reaching the sample as well as the sample density and chemical structure. The largest source of systematic uncertainty comes from the calculated muon stopping distributions, corresponding to a maximum 3% uncertainty in mean implantation depth.[26] In the microwave cavity perturbation measurements, the piece of $Ba(Co_{0.074}Fe_{0.926})_2As_2$ was mounted on a temperature-controlled sapphire plate, and a 942 MHz loop-gap resonator, described in detail elsewhere,[8] was used to obtain $\Delta\lambda(T)$.

Figure 1 shows typical μSR precession signals obtained with a small transverse magnetic field of 4.7 mT applied perpendicular to both the initial muon-spin polarization and beam direction, but parallel to the *ab* face of the crystal. The top panel shows the precession signal [at a frequency $\nu = \gamma_\mu B/(2\pi)$, where $\gamma_\mu = 2\pi \times 135.54$ MHz/T is the muon gyromagnetic ratio] in the normal state where the mean internal field is equal to the applied field. Signals taken below T_c are shown in the bottom panel. All measurements were made after cooling in zero field and then applying the external field at 4 K parallel to the *ab* plane. Changes in the low-temperature signal are evident in the raw spectra. In particular, note the reduction in the average frequency in the superconducting state due to Meissner screening. Also, the bottom panel clearly shows the frequency shift is larger at the higher implantation energy of 21.3 keV (corresponding to a mean implantation depth of 99 nm) compared to 5 keV (mean implantation depth of 27.4 nm). All the data in the superconducting state were analyzed assuming a modified London model profile,[22]

$$B(z) = \begin{cases} B_0 \exp(-\frac{z-d}{\lambda}), & z \geqslant d, \\ B_0, & z < d, \end{cases} \quad (1)$$

where B_0 is the magnitude of the applied field, λ is the in-plane magnetic penetration depth, z is the depth below the surface, and d is an effective layer closest to the surface in which shielding currents are suppressed. The same effect has been reported previously in YBCO films and crystals and attributed to surface roughness on the ~80 mm^2 sample.[22,27] However, this does not mean that the surface is chemically distinct or nonsuperconducting, but rather that there is a rough surface region which cannot carry the full supercurrent response. A theoretical muon-spin precession signal $A(t)$ was generated for each z and then averaged over the stopping distribution $\zeta(z)$,

$$A(t) = A_0 \exp\left[-\frac{(\sigma t)^2}{2}\right] \int dz\, \zeta(z) \cos[\gamma_\mu B(z) t + \varphi], \quad (2)$$

where A_0 is the initial amplitude detected. The Gaussian depolarization rate σ is a fit parameter which allows for any inhomogeneous broadening due to nuclear dipole moments and lateral variations in d. Below T_c, $\sigma = 0.33(4)$ μs^{-1} appears to be almost independent of temperature and beam energy. More details on the analysis can be found in Refs. 22 and 28. The fitted curves are shown in Fig. 1.

Figure 2 shows the average local field $[\langle B \rangle = \int \zeta(z) B(z) dz]$ as a function of the beam energy. The data are consistent with an exponential decrease as a function of increasing depth, as expected from a local superconductor. The curve in Fig. 2 is derived from a global fit for all energies with the corresponding implantation profiles (two examples shown as insets). The data points result from single-energy fits using the modified London model. The close agreement implies the model provides an excellent fit to the experimental data. The common parameters derived from the global fit are $\lambda(T = 4\text{ K}) = 252(2)$ nm and $d = 14.5(9)$ nm where the given uncertainties are purely statistical. Similar results were obtained at a magnetic field of 2.5 mT, where $\lambda(T = 4\text{ K}) = 258(2)$ nm, indicating there is little field dependence in λ. There is no evidence for the paramagnetism that has been observed by bulk μSR in the vortex state.[29]

The temperature dependences of λ measured with LE-μSR are shown as the solid diamonds in Fig. 3(a). The data points were obtained at a single energy of 21.3 keV, with d fixed to the value determined from the global fit at $T = 4$ K (Fig. 2). Microwave cavity perturbation measurements of $\Delta\lambda(T)$ were

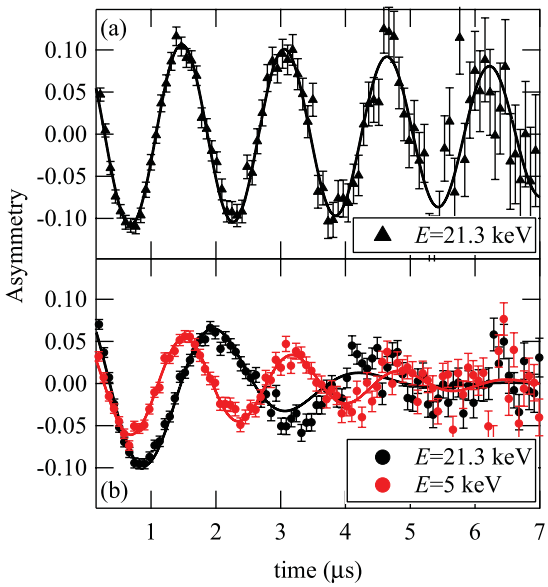

FIG. 1. (Color online) Muon-spin-precession signals in $Ba(Co_{0.074}Fe_{0.926})_2As_2$ in an applied field of $\mu_0 H = 4.7$ mT, (a) in the normal state at $T = 25$ K and (b) in the superconducting state at $T = 4$ K with $E = 5$ keV and 21.3 keV. The solid lines represent fits to a London model as described in the text.

made on a piece of the same crystal, which was cleaved on both sides [red (small light gray) square points in Fig. 3(a)]. It is clear the two methods are in excellent agreement below 13 K. One can use the microwave data to extrapolate the 4 K μSR measurement to obtain $\lambda(0) = 250.2(2.6)$ nm. By taking into account ~3 % uncertainties resulting from the muon stopping profiles, the error on $\lambda(0)$ grows to ~8 nm. Above 13 K there is some difference between the two methods which we attribute to flux penetration in the μSR experiment as one approaches T_c and the applied magnetic field of 4.67 mT exceeds the effective lower critical field for flux penetration. Note the temperature dependence of λ at low temperatures is similar to recent TDR results [blue (dark gray) squares in Fig. 3][20] on a thin sample but is considerably weaker than in previous

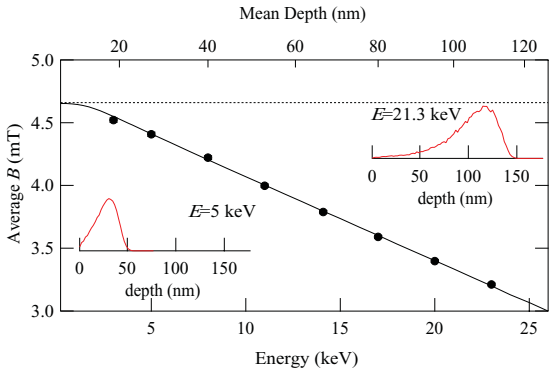

FIG. 2. (Color online) The average magnetic field vs the muon energy at $T = 4$ K with an applied field $\mu_0 H = 4.67$ mT (dotted line). The solid line has been obtained by a global fit to the data at all energies. The insets show the calculated stopping distributions of the muons at implantation energies of 5 keV and 21.3 keV.

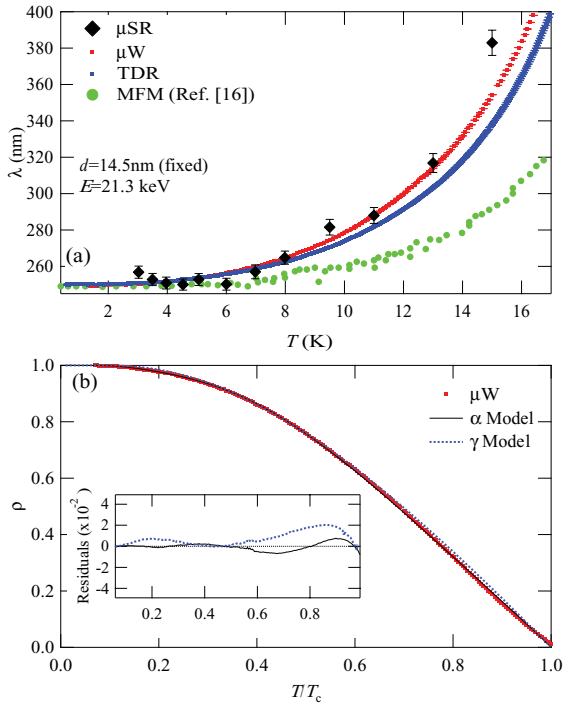

FIG. 3. (Color online) (a) The temperature dependence of λ. The black diamonds are measurements of the absolute value of λ from LE-μSR whereas the small (red/light gray) squares are from microwave cavity perturbation on a piece of the same crystal shifted to overlap with the LE-μSR data at low temperature. For comparison, we also show TDR (blue/dark gray squares) and MFM (green/gray circles) results for $\Delta\lambda(T)$, all shifted to agree at $T = 0$. The TDR and microwave error bars are smaller than the symbols. (b) The normalized superfluid density ρ plotted versus T/T_c. The solid black (dotted blue/dark gray) line is a fit to the α (γ) model. The inset shows the difference between the fitted curve and the experimental data.

studies on thicker crystals.[19] This suggests that early studies may have been affected by anomalous temperature-dependent field penetration from the c-axis edges. It is interesting to note that these results show stronger T dependence than found by MFM [shown in Fig. 3(a) (Ref. 16) as large green circles]. One difference is that the present measurements, as well as previous TDR results, measure an average over the surface whereas MFM is a pointlike probe. Such differences between methods and crystals indicate there are considerable variations in the spectrum of low-energy excitations depending on doping and/or surface quality. Clearly these results underscore the need to repeat measurements on the same crystal with several methods to be certain about the temperature dependence of the intrinsic superfluid density.

Microwave measurements are very precise but are insensitive to the absolute value of λ, and also have some uncertainty associated with the field profile which must be assumed. Combining microwave measurements with LE-μSR reduces these uncertainties and allows one to determine the superfluid density and its variation as a function of temperature with a high confidence level. The temperature dependence of the superfluid density normalized to zero temperature is shown in Fig. 3(b). The data is very well fitted using a phenomenological

two-gap s-wave model ("α model"),[30] where

$$\rho(T) = \left(1 + \frac{\Delta\lambda(T)}{\lambda(0)}\right)^{-2}$$
$$= 1 - y\frac{\delta n_s[\Delta_S(T),T]}{n_s(0)} - (1-y)\frac{\delta n_s[\Delta_L(T),T]}{n_s(0)}$$

$$\frac{\delta n_s[\Delta_i(T),T]}{n_s(0)} = \frac{2}{k_B T}\int_0^\infty f[\varepsilon,\Delta_i(T),T] \times \{1 - f[\varepsilon,\Delta_i(T),T)]\}d\varepsilon,$$

and

$$\Delta_{L,S}(T) = \Delta_{L,S}(0)\tanh\left[\frac{\pi k_B T_c}{\Delta_{L,S}(0)}\sqrt{a_{L,S}\left(\frac{T_c}{T} - 1\right)}\right].$$

Here, the subscript $i = L$ denotes the larger gap which is more apparent at high temperatures, close to T_c, and $i = S$ the smaller gap which dominates at low temperature; $0 \leqslant y \leqslant 1$ determines the respective contributions to the superfluid density, where we find $y = 0.097(1)$. The function $f[\varepsilon,\Delta_i(T),T]$ is the Fermi-Dirac distribution at energy ε and gap Δ. The free parameter $a_{L,S}$ describes phenomenologically the shape of the gaps, e.g., $a_{L,S} \equiv 1$ in the BCS limit; for the small gap we define $a_S = 1$ (Ref. 17) and find $a_L = 0.83(3)$. We find the large gap $2\Delta_L(0)/k_B T_c = 3.46(0.10)$ is close to the BCS weak-coupling limit whereas the small gap amounts to $2\Delta_S(0)/k_B T_c = 1.20(7)$. These parameters are also close to those derived from vortex-state μSR measurements.[31] This is somewhat surprising given the high degree of vortex lattice disorder and the field-induced magnetism.[11] The BCS-like component is also consistent with those found in the hole-doped $Ba_{0.68}K_{0.32}Fe_2As_2$.[32] The data were also analyzed using a self-consistent two-gap model which takes into account the interaction between bands ("γ model").[33] The quality of the fit is similar to the phenomenological two-gap model over the full temperature range and the derived gap parameters are about 10% larger. A comparison of the residuals between the data and the two fitting functions is shown in the inset of Fig. 3(b). It is clear that both are very good fits. Below 12 K, one can also parametrize the data in terms of a power law, where $\rho = 1 - \alpha(T/T_c)^n$; we obtain $n = 2.51(2)$ and $\alpha = 1.39(3)$, where the uncertainties represent the deviation in the parameters as the upper limit of the fitting range is varied between 5 K and 12 K. These are similar to but more precise than earlier reports.[17–20] Such power-law behavior is consistent with that expected from a fragmented Fermi surface with multiple gaps[34] since the low limit of the temperature range is not much less than the smaller gap. Although there is now broad agreement between LE-μSR, bulk μSR, microwave, and TDR methods near this concentration, the MFM results[16] find a much weaker temperature dependence in $\Delta\lambda$ as shown in Fig. 3(a). This method is unique in that it probes the behavior of λ in a micrometer-sized region of the surface whereas all of the other methods average over a much larger region of the crystal. This might explain some of the differences, however, the MFM results appear to be independent of position at this doping.

In conclusion, we have investigated the magnetic field penetration in the Meissner state of freshly cleaved $Ba(Co_{0.074}Fe_{0.926})_2As_2$ using both LE-μSR and microwave cavity perturbation. The absolute value of λ extrapolated to $T = 0$ is 250(8) nm, where most of this uncertainty originates from the muon stopping distribution. The temperature dependence of the superfluid density fits well to a two-gap s-wave model over the full temperature range. We have shown that there is broad agreement between LE-μSR, microwaves, and TDR results.

The μSR measurements were performed at the Swiss Muon Source, Paul Scherrer Institute, Villigen, Switzerland. This work was supported by NSERC and the US Department of Energy, Office of Basic Energy Science, Division of Materials Sciences and Engineering. Ames Laboratory is operated for the US Department of Energy by Iowa State University under Contract No. DE-AC02-07CH11358.

*oren@triumf.ca

†Present address: KTH Royal Institute of Technology, ICT Material Physics, Electrum 229, 164 40 Kista, Sweden.

[1] Y. Kamihara, T. Watanabe, M. Hirano, and H. Hosono, J. Am. Chem. Soc. **130**, 3296 (2008).

[2] X. H. Chen, T. Wu, G. Wu, R. H. Liu, H. Chen, and D. F. Fang, Nature (London) **453**, 761 (2008).

[3] H. Wadati, I. Elfimov, and G. A. Sawatzky, Phys. Rev. Lett. **105**, 157004 (2010).

[4] H. Luetkens, H.-H. Klauss, M. Kraken, F. J. Litterst, T. Dellmann, R. Klingeler, C. Hess, R. Khasanov, A. Amato, C. Baines, M. Kosmala, O. J. Schumann, M. Braden, J. Hamann-Borrero, N. Leps, A. Kondrat, G. Behr, J. Werner, and B. Buchner, Nat. Mater. **8**, 305 (2009).

[5] R. T. Gordon, H. Kim, N. Salovich, R. W. Giannetta, R. M. Fernandes, V. G. Kogan, T. Prozorov, S. L. Bud'ko, P. C. Canfield, M. A. Tanatar, and R. Prozorov, Phys. Rev. B **82**, 054507 (2010).

[6] Johnpierre Paglione and Richard L. Greene, Nat. Phys. **6**, 645 (2010).

[7] K. Ishida, Y. Nakai, and H. Hosono, J. Phys. Soc. Jpn. **78**, 062001 (2009).

[8] W. N. Hardy, D. A. Bonn, D. C. Morgan, R. Liang, and K. Zhang, Phys. Rev. Lett. **70**, 3999 (1993).

[9] J. E. Sonier, R. F. Kiefl, J. H. Brewer, D. A. Bonn, J. F. Carolan, K. H. Chow, P. Dosanjh, W. N. Hardy, R. Liang, W. A. MacFarlane, P. Mendels, G. D. Morris, T. M. Riseman, and J. W. Schneider, Phys. Rev. Lett. **72**, 744 (1994).

[10] J. E. Sonier, J. H. Brewer, and R. F. Kiefl, Rev. Mod. Phys. **72**, 769 (2000).

[11] J. E. Sonier, W. Huang, C. V. Kaiser, C. Cochrane, V. Pacradouni, S. A. Sabok-Sayr, M. D. Lumsden, B. C. Sales, M. A. McGuire, A. S. Sefat, and D. Mandrus, Phys. Rev. Lett. **106**, 127002 (2011).

[12] H. Saadaoui, W. A. MacFarlane, Z. Salman, G. D. Morris, Q. Song, K. H. Chow, M. D. Hossain, C. D. P. Levy, A. I. Mansour, T. J.

Parolin, M. R. Pearson, M. Smadella, D. Wang, and R. F. Kiefl, Phys. Rev. B **80**, 224503 (2009).

[13]A. S. Sefat, R. Jin, M. A. McGuire, B. C. Sales, D. J. Singh, and D. Mandrus, Phys. Rev. Lett. **101**, 117004 (2008).

[14]J. K. Dong, S. Y. Zhou, T. Y. Guan, X. Qiu, C. Zhang, P. Cheng, L. Fang, H. H. Wen, and S. Y. Li, Phys. Rev. B **81**, 094520 (2010).

[15]J. P. Reid, M. A. Tanatar, X. G. Luo, H. Shakeripour, N. Doiron-Leyraud, N. Ni, S. L. Bud'ko, P. C. Canfield, R. Prozorov, and L. Taillefer, Phys. Rev. B **82**, 064501 (2010).

[16]L. Luan, O. M. Auslaender, T. M. Lippman, C. W. Hicks, B. Kalisky, J. H. Chu, J. G. Analytis, I. R. Fisher, J. R. Kirtley, and K. A. Moler, Phys. Rev. B **81**, 100501(R) (2010).

[17]L. Luan, T. M. Lippman, C. W. Hicks, J. A. Bert, O. M. Auslaender, J. H. Chu, J. G. Analytis, I. R. Fisher, and K. A. Moler, Phys. Rev. Lett. **106**, 067001 (2011).

[18]J. S. Bobowski, J. C. Baglo, J. Day, P. Dosanjh, R. Ofer, B. J. Ramshaw, R. Liang, D. A. Bonn, W. N. Hardy, H. Luo, Z.-S. Wang, L. Fang, and H.-H. Wen, Phys. Rev. B **82**, 094520 (2010).

[19]R. T. Gordon, N. Ni, C. Martin, M. A. Tanatar, M. D. Vannette, H. Kim, G. D. Samolyuk, J. Schmalian, S. Nandi, A. Kreyssig, A. I. Goldman, J. Q. Yan, S. L. Bud'ko, P. C. Canfield, and R. Prozorov, Phys. Rev. Lett. **102**, 127004 (2009).

[20]H. Kim, R. T. Gordon, M. A. Tanatar, J. Hua, U. Welp, W. K. Kwok, N. Ni, S. L. Bud'ko, P. C. Canfield, A. B. Vorontsov, and R. Prozorov, Phys. Rev. B **82**, 060518 (2010).

[21]N. Ni, M. E. Tillman, J.-Q. Yan, A. Kracher, S. T. Hannahs, S. L. Bud'ko, and P. C. Canfield, Phys. Rev. B **78**, 214515 (2008).

[22]R. F. Kiefl, M. D. Hossain, B. M. Wojek, S. R. Dunsiger, G. D. Morris, T. Prokscha, Z. Salman, J. Baglo, D. A. Bonn, R. Liang, W. N. Hardy, A. Suter, and E. Morenzoni, Phys. Rev. B **81**, 180502(R) (2010).

[23]T. Prokscha, E. Morenzoni, K. Deiters, F. Foroughi, D. George, R. Kobler, A. Suter, and V. Vrankovic, Nucl. Instrum. Methods A **595**, 317 (2008).

[24]E. Morenzoni, H. Glückler, T. Prokscha, H.-P. Weber, E. M. Forgan, T. J. Jackson, H. Luetkens, Ch. Niedermayer, M. Pleines, M. Birke, A. Hofer, J. Litterst, T. Riseman, and G. Schatz, Physica B **289-290**, 653 (2000).

[25]W. Eckstein, *Computer Simulation of Ion-Solid Interactions* (Springer, Berlin, 1991).

[26]E. Morenzoni, H. Gluckler, T. Prokscha, R. Khasanov, H. Luetkens, M. Birke, E. M. Forgan, Ch. Niedermayer, and M. Pleines, Nucl. Instrum. Methods B **192**, 254 (2002).

[27]T. J. Jackson, T. M. Riseman, E. M. Forgan, H. Glückler, T. Prokscha, E. Morenzoni, M. Pleines, Ch. Niedermayer, G. Schatz, H. Luetkens, and J. Litterst, Phys. Rev. Lett. **84**, 4958 (2000).

[28]B. M. Wojek, Ph.D. thesis, University of Zurich, 2011, http://dx.doi.org/10.5167/uzh-57024.

[29]T. J. Williams, A. A. Aczel, E. Baggio-Saitovitch, S. L. Bud'ko, P. C. Canfield, J. P. Carlo, T. Goko, H. Kageyama, A. Kitada, J. Munevar, N. Ni, S. R. Saha, K. Kirschenbaum, J. Paglione, D. R. Sanchez-Candela, Y. J. Uemura, and G. M. Luke, Phys. Rev. B **82**, 094512 (2010).

[30]F. Bouquet, Y. Wang, R. A. Fisher, D. G. Hinks, J. D. Jorgensen, A. Junod, and N. E. Phillips, Europhys. Lett. **56**, 856 (2001).

[31]T. J. Williams, A. A. Aczel, E. Baggio-Saitovitch, S. L. Bud'ko, P. C. Canfield, J. P. Carlo, T. Goko, J. Munevar, N. Ni, Y. J. Uemura, W. Yu, and G. M. Luke, Phys. Rev. B **80**, 094501 (2009).

[32]Z. Li, D. L. Sun, C. T. Lin, Y. H. Su, J. P. Hu, and G.-Q. Zheng, Phys. Rev. B **83**, 140506(R) (2011).

[33]V. G. Kogan, C. Martin, and R. Prozorov, Phys. Rev. B **80**, 014507 (2009).

[34]A. B. Vorontsov, M. G. Vavilov, and A. V. Chubukov, Phys. Rev. B **79**, 140507(R) (2009).